Possible Role of Contact Following in the Generation of Coherent Motion of Dictyostelium Cells

Umeda, Tamiki

Inouye, Kei

(Citation)
Journal of Theoretical Biology,219(3):301-308

(Issue Date)
2002-12-07

(Resource Type)
journal article

(Version)
Accepted Manuscript

(URL)
https://hdl.handle.net/20.500.14094/90000253

Possible Role of Contact Following in the Generation of Coherent Motion of *Dictyostelium* Cells

Tamiki Umeda [a,*], Kei Inouye [b]

[a] *Department of Marine Engineering, Kobe University of Mercantile Marine, Kobe 658-0022, Japan*

[b] *Department of Botany, Division of Biological Science, Graduate School of Science, Kyoto University, Kyoto 606-8502, Japan*

Abstract

After aggregation by chemotaxis, cells of the cellular slime mold *Dictyostelium discoideum* form a multicellular structure and show coherent motion such as vortices. Here we present a mathematical model to explain both aggregation and coherent motion of cells in two-dimensional space. The model incorporates chemotactic response of cells and the cell's property, called "contact following", to follow the other cells with which they are in contact. Analytical study and computer simulation using the model show that with contact following cells form circular clusters within which cell rotation occurs. Unidirectional cell motion in a long belt of cells is another type of solution of the model. Besides, contact following has an effect to accelerate cell cluster merging. By considering the mechanism of cell movement, possible explanations of contact following are proposed.

1 Introduction

The study of self-organizing systems composed of motile elements is a fascinating field of interests. A variety of living things such as birds, fish, slime molds, and bacteria exhibit characteristic patterns of collective movement. The self-organized motion of a swarm of social amoebae is of particular interest because the behavior of individual amoebae and the underlying molecular mechanisms are well characterized.

* Corresponding author.
emai: umeda@cc.kshosen.ac.jp

After the vegetative growing phase, solitary amoebae of *Dictyostelium discoideum* aggregate to become multicellular by chemotaxis towards cyclic AMP. The organized movement of *Dictyostelium* cells during aggregation has been a subject of extensive studies, both experimental and theoretical, and we now know about its mechanism in great detail (Höfer *et al.*, 1995; Dallon & Othmer, 1997; for reviews see: Parent & Devreotes, 1999; Kessin, 2001). Although the chemotactic ability peaks at the aggregation stage, it is retained throughout the multicellular phase and thought to play important roles in the morphogenetic movements during this period as well (Dormann *et al.*, 2000). However, chemotaxis is not the only component that rules the collective movement of *Dictyostelium* cells. During and after aggregation, cells exhibit a striking tendency to follow the other cells with which they are in contact. For example, a cell coming into contact with the side of a stream of aggregating cells is guided in the direction of the flow only after it touches the back end of a cell in the stream (Shaffer 1964). Cells at the multicellular stages seem to have an even stronger predisposition to follow the preceding cells. On close observation, it is evident that such cells continuously extend their pseudopod towards the retracting end of the preceding cells, suggesting that this behavior is not directly caused by mechanical forces such as cell adhesion but requires active cell movement (Inouye, 1977). A study using mutant strains showing no chemotactic response to any of the known chemoattractants indicates that this tendency is independent of chemotaxis (Ohtsuka, 1994). This property known as "contact following" (Shaffer, 1962), has not been paid due attention, however, and its possible roles in the organization of cell movements remain unexplored.

In this study, we have examined how the pattern of coordinated cell movement is modulated by chemotaxis and contact following. For this purpose, the relay reaction of chemotactic signals, which by itself can generate coordinated cell movements such as rotational motion (Durston, 1973; Tyson *et al.*, 1989; Pálsson & Cox, 1996), is not incorporated in the model. In our model, the magnitude of the propulsive force of individual cells is fixed while its direction is determined by the concentration gradient of a diffusible chemical (chemotaxis) and local interaction with the surrounding cells (contact following). In normal development, *Dictyostelium* cells form three-dimensional motile tissues which exhibit coordinated cell motion, but when confined in two-dimensional space, they can still aggregate normally and show movement patterns characteristic of the multicellular stage (Bonner, 1998). Rotational and unidirectional movements of cell clusters are common under such circumstances and has recently been a subject of experimental and numerical simulation studies (Nicol *et al.*, 1999; Rappel *et al.*, 1999). In the present paper, we examine under what conditions coordinated movements of cells such as vortices are generated in two-dimensional space using analytical and numerical methods.

2 Model

The model is based on our previous models for the movement of cell aggregates (Inouye & Takeuchi, 1979; Umeda, 1989; Umeda & Inouye, 1999), in which a cell at position $\mathbf{x}_i$ generates motive force $\mathbf{f}_i$ against resistance force which is assumed to be proportional to their velocity $\mathbf{v}_i = d\mathbf{x}_i/dt$. This resistance force is considered to be a sum of the resistance due to the viscoelasticity of the cytoplasm and the force needed to break the adhesion to the neighboring cells and the substratum (see Umeda & Inouye, 1999 for further discussion). We assume that the cell receives an additional force $\mathbf{T}_i$ from the surrounding cells if in a packed aggregate so that the cell density ρ of such aggregates is fixed at ρ_0. Since the forces are balanced, the following equation holds for each cell:

$$\mathbf{f}_i - a\mathbf{v}_i + \mathbf{T}_i = 0, \tag{1}$$

where a is constant. The inertia force can be neglected because of the very small size and low speed of cells. Furthermore, since there is no slip between the lateral sides of cohesive cells, no viscous force acts between cells (Umeda & Inouye, 1999). For isolated cells, $\rho < \rho_0$ and the force $\mathbf{T}_i$ vanishes.

The magnitude of the motive force is assumed to be constant (f_0) and its direction dependent on the gradient of a chemical substance, whose concentration at position $\mathbf{x}$ and time t is denoted by $c(\mathbf{x}, t)$. Isolated cells generate constant motive force in the direction of the gradient of c, that is, $\mathbf{f}_i = f_0 \nabla c / |\nabla c|$. When in contact with other cells, $\mathbf{f}$ is deviated by the effect of contact following. Although this effect depends on the velocity and configuration of the surrounding cells, we here assume for mathematical simplicity that the direction of motive force is influenced by the mean velocity $\langle \mathbf{v} \rangle_i$ of the surrounding cells. The arithmetic average of the effects of chemotaxis and contact following gives

$$\mathbf{f}_i = f_0 \frac{\nabla c + b\langle \mathbf{v} \rangle_i}{|\nabla c + b\langle \mathbf{v} \rangle_i|}, \tag{2}$$

where b is a constant representing the relative contribution of contact following.

The chemical substance is assumed to be secreted by individual cells and decay at a constant rate. So, the changes in c may be described by the following equation:

$$\frac{\partial c}{\partial t} = k_1 \sum_i \delta(\mathbf{x} - \mathbf{x}_i) - k_2 c + D \triangle c, \tag{3}$$

where $\delta(\mathbf{x}-\mathbf{x}_i)$ denotes Dirac's delta function, and k_1, k_2 and D are constants.

We derive the continuous model by treating cell density as a continuous function $\rho(\mathbf{x}, t)$ and cell velocity as $\mathbf{v}(\mathbf{x}, t)$. Then equation (3) is rewritten as

$$\frac{\partial c}{\partial t} = k_1\rho - k_2 c + D\triangle c. \tag{4}$$

Substituting (2) into (1) and averaging it over a small area at position $\mathbf{x}$ give

$$f_0\frac{\nabla c + b\mathbf{v}}{|\nabla c + b\mathbf{v}|} - a\mathbf{v} - \frac{1}{\rho}\nabla p = 0, \tag{5}$$

where $\langle\mathbf{v}\rangle_i$ was identified with $\mathbf{v}$. The last term of the left-hand side of (5) is expressed in the form of the gradient of pressure p (Umeda, 1989). In packed aggregates, the velocity field $\mathbf{v}$ satisfies

$$\nabla\cdot\mathbf{v} = 0, \tag{6}$$

since the cell density is constant everywhere. For isolated cells (i.e., $\rho < \rho_0$), $p = 0$, $b = 0$, and eqn (6) is replaced with

$$\frac{\partial\rho}{\partial t} + \nabla\cdot(\rho\mathbf{v}) = 0. \tag{7}$$

3 Stationary solution

3.1 ROTATIONAL MOVEMENT

Stationary solutions of the above model can be obtained under spatial symmetry conditions. We first consider the situation where cells are gathered to form a circular aggregate of radius R, and assume that $\mathbf{v}$, c and p are functions of the radial distance r from the center of the circle. Then the cell density is $\rho = \rho_0$ $(r \le R)$ and $\rho = 0$ $(r > R)$, and the stationary solution of (4) is given by

$$c(r) = \begin{cases} \alpha\left[1 - \beta R\, K_1(\beta R) I_0(\beta r)\right] & (r \le R) \\ \alpha\beta R\, I_1(\beta R) K_0(\beta r) & (r > R), \end{cases} \tag{8}$$

where $\alpha = k_1\rho_0/k_2$, $\beta = \sqrt{k_2/D}$, and I_0, I_1, K_0, K_1 are modified Bessel functions. Since $v_r = 0$ from (6), azimuthal velocity v_θ is obtained by solving

the azimuthal component of (5):

$$v_\theta(r) = 0, \quad \pm\sqrt{\left(\frac{f_0}{a}\right)^2 - \left(\frac{1}{b}\frac{dc}{dr}\right)^2}. \tag{9}$$

If $|dc/dr| > bf_0/a$, v_θ takes only the value zero and cells come to a standstill. However, as $|dc/dr|$ becomes smaller than bf_0/a, there are two non-zero values besides $v_\theta = 0$ and clockwise or counterclockwise cell rotation emerges. Since eqn (8) indicates that dc/dr is a decreasing function of r in $0 \leq r \leq R$ and zero at $r = 0$, all cells rotate if $dc/dr|_{r=R} > -bf_0/a$ holds. Otherwise, only cells within the central part of the aggregate rotate. The radial component of eqn (5) then gives the equation for the pressure. Substituting (9), we have

$$\frac{dp}{dr} = \begin{cases} -\rho_0 f_0 \text{ if } \frac{dc}{dr} < -\frac{bf_0}{a} \\ \frac{\rho_0 a}{b}\frac{dc}{dr} \quad \text{otherwise.} \end{cases} \tag{10}$$

Solving (10) with the boundary condition $p(R) = 0$ gives the pressure distribution at steady state.

Figure 1 shows an example of stationary solution for c, v_θ and p against r. In this case, cells within the central part of the aggregate rotate.

3.2 UNIDIRECTIONAL MOVEMENT

We next consider the case in which cells form a belt-shaped aggregate of a uniform width and move straight within it. Cell density is assumed to be independent of x, and $\rho = \rho_0$ for $-d \leq y \leq d$ and $\rho = 0$ otherwise (Fig. 2). Then the stationary distribution of c becomes

$$c(y) = \begin{cases} \alpha\left[1 - e^{-\beta d}\cosh(\beta y)\right] & (-d \leq y \leq d) \\ \alpha \sinh(\beta d) e^{\pm\beta y} & (|y| > d). \end{cases} \tag{11}$$

The concentration profile of $c(y)$ is similar to the one for the rotationally symmetric solution. Assuming $v_y = 0$, eqns (5) and (6) give

$$v_x(y) = 0, \quad \pm\sqrt{\left(\frac{f_0}{a}\right)^2 - \left(\frac{1}{b}\frac{dc}{dy}\right)^2}. \tag{12}$$

Therefore, cells would move rightward or leftward along the x-axis. Cell speed has a maximum at $y = 0$ and decreases with $|y|$. If $|dc/dy| > bf_0/a$ at $y = \pm d$, only the cells within an inner zone move.

4 Numerical simulation

To verify whether the cell population starting from random distribution reaches the above stationary states, we numerically calculate the cell motions using eqns (1)-(3). The calculation was performed using a hybrid method of particle method and finite difference method (Dallon & Othmer, 1997). On a square region of size 1 with periodic boundary conditions, the location of cells is updated according to $\mathbf{x}_i(t + \Delta t) = \mathbf{x}_i(t) + \mathbf{v}_i \Delta t$. Simultaneously, (3) is solved using the Euler explicit method, in which the term including $\delta(\mathbf{x} - \mathbf{x}_i)$, lagged in time, is interpolated to the nearest grid points. Then ∇c at the location of each cell is calculated from the values on the grid points. For the mean velocity $\langle \mathbf{v} \rangle_i$ at position $\mathbf{x}_i$, we use a weighted mean of surrounding $\mathbf{v}_j$ with lagged time. The most difficult point is the calculation of $\mathbf{T}_i$. To do this, we used a method similar to the MPS method (moving particle semi-implicit method), which was originally developed by Koshizuka *et al.* (1996) to solve the free boundary problem of incompressible viscous flow. Using a weight function $w(r) = r_e/r - 1$ $(r \leq r_e)$ and 0 $(r > r_e)$, we define the cell density at the location of the i-th cell as $\rho_i = (1/\omega) \sum_{j \neq i} w(|\mathbf{x}_j - \mathbf{x}_i|)$, where ω is an empirical constant. The term $\mathbf{T}_i$ is replaced with a continuous function $-(1/\rho_0)\nabla p$, and then $p_i = p(\mathbf{x}_i)$ for each cell is calculated by solving the simultaneous equations derived from the incompressibility condition. Then $(1/\rho_0)\nabla p$ is calculated using the values of p_i's and $\mathbf{x}_i$'s. In this method, the motion of isolated cells can easily be treated as well; we merely put $p_i = 0$ for the cells that satisfy $\rho_i < (1 - \epsilon)\rho_0$ with small ϵ. We also put $b = 0$ for $\rho_i < (1 - \epsilon')\rho_0$ where $\epsilon' > \epsilon$ so that the cells on the boundary of the aggregate are active in contact following. Detailed description of the numerical method will be presented elsewhere.

Figure 3 shows snapshots of a simulation started with randomly distributed cells with $\mathbf{v}_i = 0$, and $c = 0$. Firstly, cells are gathered to form small clusters, and then clusters merge to form larger clusters (Fig. 3(a)). As clusters grow to a certain extent, cells come to rotate within them. Nevertheless, when a cluster is going to merge with another cluster, cells do not rotate but move in the direction of the other cluster (Fig. 3(b)). By time $t = 1.5$, two circular clusters are formed (Fig. 3(c)-(d)). In the larger cluster, only the cells in its central part rotate vigorously, but in the smaller one all cells rotate. The values of v_θ for cells within the larger cluster are plotted in Fig. 1(b). They roughly agree with the rotationally symmetric solution of the continuous model, indicating that the cluster is almost in the stationary state of our model. However, the outer cells in the simulation rotate at a low velocity unlike the result of continuous

model. This may be caused by the small number of total cells and the finite size of cell-cell interaction range in the simulation.

Several calculations with various b showed similar results, but cells did not rotate when $b = 0$. Increasing b accelerated cluster merging as well as cell rotation (Fig. 4). This acceleration can be understood as a result of the coherent cell motion toward other clusters. However, further increase of this parameter destabilized the central symmetry of cell motion to give the non-uniform, rotational movement of deformed cluster. The question of why this type of instability occurs is still open, but it may be interesting because the symmetry breaking from the rotating state is often observed in real two-dimensional aggregates of slime mold amoebae.

The unidirectional stationary movement of cells had not been seen in the simulation started with randomly distributed cells. However, when the initial distribution of cells was arranged appropriately, such movements were obtained in numerical calculations for some parameter values. This suggests that there may be stable stationary solutions corresponding to unidirectional movement at least with periodic boundary conditions.

5 Discussion

Since the aim of the present study was to know how contact following affects the movement pattern of cells, the simple forms of chemotaxis (eqn (2)) and reaction kinetics of the chemotactic substance (eqn (3)) were postulated. The main conclusions do not depend on this specific formulation of the model, although the spatial distributions of the chemoattractant and cell speed shown in Fig. 1 may be slightly different. The model can be adapted to incorporate other forms of chemotaxis, or even to situations where cells are held together by non-chemotactic force such as cell adhesion. For instance, in the case of the circular aggregate considered above, if the cells have a tendency $\mathbf{u}$ to move towards the centre of the aggregate, the motive force may be written in the form $\mathbf{f} = f_0(\mathbf{u} + b\mathbf{v})/|\mathbf{u} + b\mathbf{v}|$. Then, bifurcation occurs at $b > b_c = ua/f_0$ to produce a rotating state. As is clear from this example, the important point of the model is the alteration of the direction of the force by the effect of contact following, and the cause of the centripetal force is not important.

We obtained two types of stationary solutions by assuming spatial symmetry. Obviously, the rotationally symmetric solution would correspond to the rotational cell movements observed in the numerical calculations and in two-dimensional aggregates of real *Dictyostelium* cells. On the other hand, the stationary solution of unidirectional movement can only be realized with periodical boundary conditions. Although this type of cell movement has not

been observed experimentally (which would be a rotating band of cells on a cylindrical surface), long lasting unidirectional movements have been obtained in numerical calculations. Its existence implies a tendency of cells to form long and thin aggregates moving in its longitudinal direction. Indeed, such movements are frequently observed in numerical calculations (see Fig. 2(b)), and also with real *Dictyostelium* cells (unpublished observations), which would account for the acceleration of cluster merging as mentioned earlier.

In eqn (2), we assumed competition between the chemotactic effect and contact following for the force generated by the cell. To asses the plausibility of this assumption, we need to consider the mechanism of cell movement. When an isolated cell moves in one direction, it extends one or more protrusions called pseudopods in the direction of its movement (Condeelis, 1993). We would argue that the direction of pseudopod elongation would determine the direction of the force generated by the cell. In the case of chemotaxis, a new pseudopod is formed in the direction the chemotactic signal comes from, which directs the force towards the signal source. If the cell is prevented by, for example, the presence of other cells from extending the pseudopod in the direction dictated by chemotaxis, the pseudopod would elongate in the direction with smaller mechanical resistance, resulting in alteration of the direction of the force vector. In a packed cell mass, the retracting tail of an adjacent cell is most likely the easiest direction for a cell to extend its pseudopod.

Obviously, this is not the only explanation of contact following, because a chain of cells with head-to-tail connection is often seen to move meandering like a snake under the two-dimensional conditions. One can envisage that the surface of the retracting tail of a cell has an ability to stimulate elongation of the pseudopod of the cell that follows it. Both mechanical means, such as "pulling" of the pseudopod surface by strong adhesion, and chemical means, such as "local chemotaxis" induced by a membrane-bound attractant, seem possible mechanisms which will be worth testing.

Recent study of Rappel *et al.* (1999) demonstrates that a group of self-propelled objects can produce a self-organized rotating state. They treated a cell as a deformable object with cohesive energy on cell-cell boundary, which would cause a cell to follow the retracting tail of an adjacent cell. This force, together with their additional assumption that the direction of the propulsive force is determined based on the interactions with the forces of neighboring cells, may produce the same effect as contact following presented here, resulting in the rotating state.

The same kind of interaction between moving objects has been considered by Levine *et al.* (2000) in their model consisting of self-propelled particles. They assumed that the self-propelling force of each particle is directional to the average velocity of the neighboring particles. Although their model does

not consider cell contact so the cell-cell interaction is long-range, and involves no chemotaxis, it also produces vortex state in the two-dimensional space. In a sense our model is an extension of this model to explain the behavior of cellular slime mold amoebae. Another model for vortex state have been presented by Ben-Jacob *et al.* (1997) to explain the collective formation of vortices by swarming bacteria. They proposed a special chemotactic response, "rotational chemotaxis", which is based on speed modulations according to the concentration of a chemoattractant. However, there is no evidence to show the existence of similar effects in cellular slime mold amoebae.

The results of the present study indicate that contact following may be playing an important role in organized cell movement in two-dimensional cell aggregates, and further suggest possible mechanisms for this phenomenon. To know whether contact following gives similar effects on cell aggregates in normal development where cells form three-dimensional aggregates, analysis of the model in three-dimensional space is required. In such cell aggregates also, concerted cell motion such as spiral movement are very common. There is strong evidence suggesting that these rotational movements are due to chemotaxis of the cells in response to rotating waves of the signaling molecule cyclic AMP (Weijer, 1999). Most theoretical models for the formation of 3-dimensional mounds are primarily based on chemotaxis, and some of them have demonstrated coherent cell motion such as rotational movement and stream formation (Vasiev et al. 1997; Pálsson and Othmer, 2000). However, it remains to be shown whether any mechanism other than the rotating chemotactic signals contributes to the generation of the coherent motion of cells. The arguments of the present study are equally applicable to three-dimensional situations, and point to the possibility that contact following plays a part in producing such coherent cell motion in three-dimensional space as well. Indeed, the present model has rotating stationary solutions in three-dimensional space with simple rotational symmetry boundary conditions. To elucidate the roles of contact following during morphogenesis, more elaborate models incorporating both contact following and signal relay would be necessary. From the experimental point of view, search for mutants with defective contact following would obviously be important.

It will also be interesting to investigate the effects of contact following on the process of cell sorting when two or more cell types differing in the properties of individual cells, such as motive force or chemotactic sensitivity; cell sorting occurs in rather straight-forward ways if contact following is not taken into account (Umeda & Inouye, 1999), but its incorporation is likely to produce more complex cell behaviors.

This research was supported in part by Grant-in-Aid for Scientific Research (c)-11837011 from Japan Society for the Promotion of Science to T.U.

References

Ben-Jacob, E., Cohen, I., Czirók, A., Vicsek, T. & Gutnick, D. L. (1997). Chemomodulation of cellular movement, collective formation of vortices by swarming bacteria, and colonial development. *Physica A* **238**, 181-197.

Bonner, J. T. (1998). A way of following individual cells in the migrating slugs of *Dictyostelium discoideum*. *Proc. Natl. Acad. Sci. USA* **95**, 9355-9359.

Condeelis, J. (1993). Life at the leading edge: The formation of cell protrusions. *Annu. Rev. Cell Biol.* **9**, 411.

Dallon, J. C. & Othmer, H. G. (1997). A discrete cell model with adaptive signalling for aggregation of *Dictyostelium discoideum*. *Phil. Trans. R. Soc. Lond. B* **352**, 391-417.

Dormann, D., Vasiev, B. & Weijer, C. J. (2000). The control of chemotactic cell movement during *Dictyostelium* morphogenesis. *Phil. Trans. R. Soc. Lond. B* **355**, 983-991.

Durston, A. J. (1973). *Dictyostelium discoideum* aggregation fields as excitable media. *J. Theor. Biol.* **42**, 483-504.

Höfer, T., Sherratt, J.A. & Maini, P.K. (1995). *Dictyostelium discoideum*: Cellular self-organization in an excitable biological medium. *Proc. R. Soc. Lond. B* **259**, 249-257.

Inouye, K. (1977). Analysis of collective movements of slime mould cells. (In Japanese). Master's Thesis, Kyoto University.

Inouye, K. & Takeuchi, I. (1979). Analytical studies on migrating movement of the pseudoplasmodium of *Dictyostelium discoideum*. *Protoplasma* **99**, 289-304.

Kessin, R. H. (2001). *Dictyostelium*. Cambridge Univ. Press, Cambridge, UK.

Koshizuka, S. & Oka, Y. (1996). Moving-particle semi-implicit method for fragmentation of incompressible fluid. *Nucl. Sci. Eng.* **123**, 421-434.

Levine, H. & Rappel, W.-J. (2000). Self-organizition in systems of self-propelled particles. *Phys. Rev. E* **63**, 17101.

Nicol, A., Rappel, W.-J., Levine, H. & Loomis, W. F. (1999). Cell-sorting in aggregates of *Dictyostelium discoideum*. *J. Cell Sci.* **112**, 3923-3930.

Ohtsuka, H. (1994). Relationship between the movements of slug cells and chemotaxis in *Dictyostelium discoideum*. (in Japanese). Master's Thesis, Kyoto University.

Pálsson, E. & Cox, E. C. (1996). Origin and evolution of circular waves and spirals in *Dictyostelium discoideum* territories. *Proc. Natl. Acad. Sci. USA* **93**, 1151-1155.

Pálsson, E. & Othmer, H. G. (2000). A model for individual and collective cell movement in *Dictyostelium discoideum*. *Proc. Natl. Acad. Sci. USA*, **97**, 10448-10453.

Parent, C. A. & Devreotes, P. N. (1999). A cell's sense of direction. *Science* **284**, 765-769 .

Rappel, W.-J., Nicol, A., Sarkissian, A., Levine, H. & Loomis, W. F. (1999). Self-organized vortex state in two-dimensional *Dictyostelium* dynamics. *Phys. Rev. Lett.* **83**, 1247-1250.

Shaffer, B. M. (1962). The Acrasina. *Adv. Morphogenesis* **2**, 109-182.

Shaffer, B. M. (1964). Intracellular movement and locomotion of cellular slime-mold amoebae. In: *Primitive motile systems in cell biology.* (R. D. Allen and N. Kamiya, Eds.), 387-405. Ac. Press, New York.

Tyson, J. J., Alexander, K. A., Manoranjan, V. S. & Murray, J. D. (1989). Spiral waves of cyclic AMP in a model of slime mold aggregation. *Physica D* **34**, 193-207.

Umeda, T. (1989). A mathematical model for cell sorting, migration and shape in the slug stage of *Dictyostelium discoideum*. *Bull. Math. Biol.* **51**, 485-500.

Umeda, T. & Inouye, K. (1999). Theoretical model for morphogenesis and cell sorting in *Dictyostelium discoideum*. *Physica D* **126**, 189-200.

Vasiev, B., Siegert, F. & Weijer, C. J. (1997). A hydrodynamic model for *D. discoideum* mound formation. *J. theor. Biol.* **184** 441-450.

Weijer, C. J. (1999). Morphogenetic cell movement in *Dictyostelium*. *Sem. Cell Dev. Biol.* **10**, 609-619.

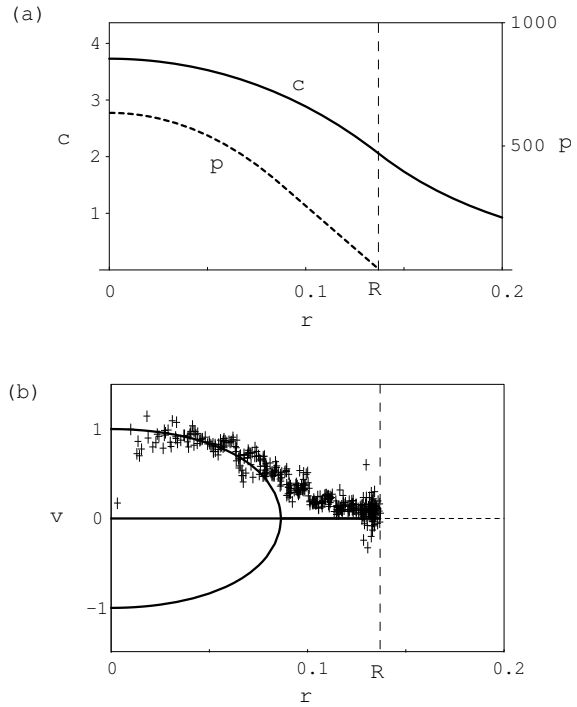

Fig. 1. The stationary, rotationally symmetric solution of the model. (a) The chemical concentration c (solid line) and the pressure p (broken line) are plotted against the radial position r. Cells are uniformly distributed within a disk of radius R. (b) The azimuthal velocity v_θ (solid line) versus r. In this case, the cells located in the region $r < r_c$ rotate clockwise ($v_\theta < 0$) or counterclockwise ($v_\theta > 0$). Pluses represent the result of the numerical calculation using eqns (1)-(3) (See also Fig. 3(d)). The parameters are $f = a = 1$, $k_1 = 0.1$, $k_2 = 100$, $D = 1$, $b = 15$, $\rho_0 = 6900$, and $R = 0.137$.

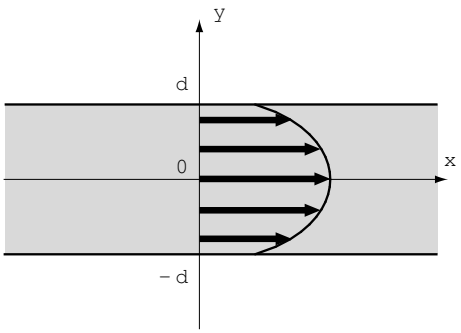

Fig. 2. Schematic representation of the stationary solution corresponding to the unidirectional movement. Cells form an infinitely long belt bounded by $y = \pm d$ (shaded zone), and move along the x-axis. Arrows indicate the velocity vector profile along the y-axis.

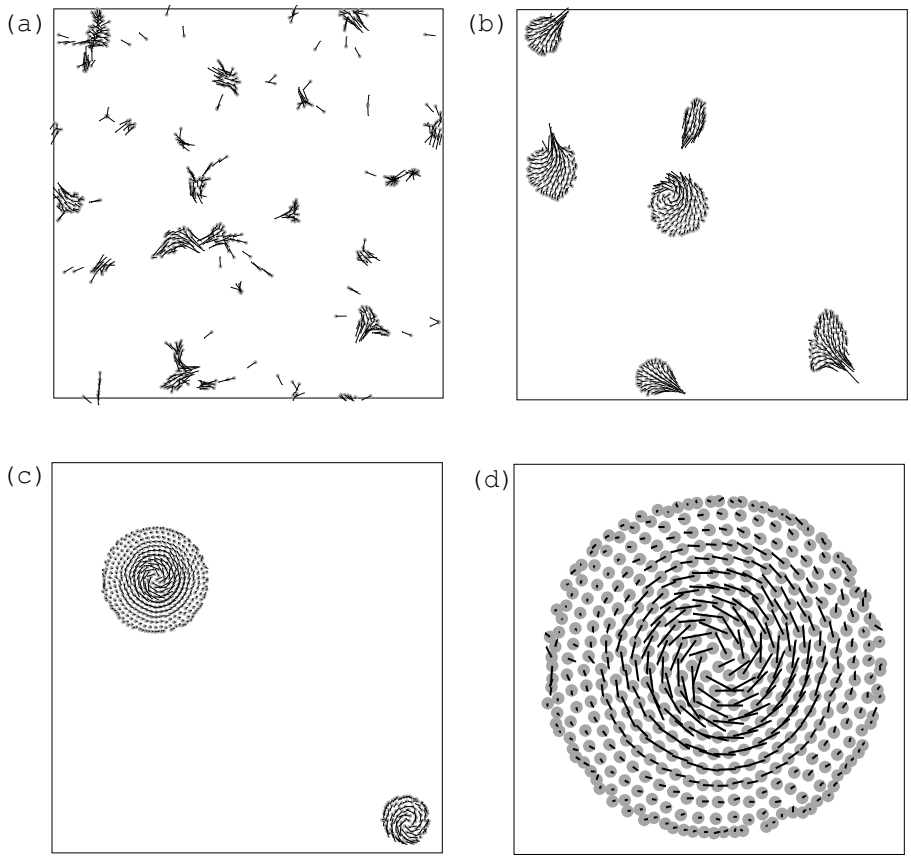

Fig. 3. A result of numerical calculation using eqns (1)-(3). Initially, 500 cells were randomly scattered in a region of size 1×1 with periodic boundary condition. The cell positions (grey circles) and velocities (lines) of the cells at the indicated times are shown. (a) $t = 0.1$. Cells are forming small clusters. The speed of isolated cells is $v = f/a$. (b) $t = 0.4$. Cell clusters merge to form larger clusters and rotational cell movement can be seen in some clusters. (c) $t = 1.5$. Two clusters of cells showing stable rotational movement. (d) Magnification of the larger cluster of (c). Cell density appears to be high at the periphery of the aggregate, but almost constant by the definition used in the calculation. Parameters are $f = a = 1$,$k_1 = 0.1$, $k_2 = 100$, $D = 1$, $b = 15$, and $\rho_0 = 6900$.

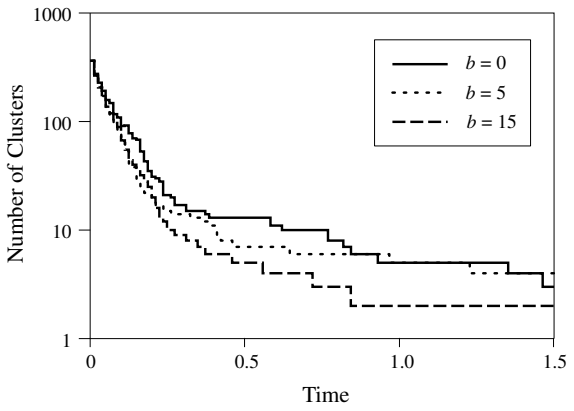

Fig. 4. Changes in the number of clusters as a function of time t. Numerical calculation was performed with various values of b, and the number of clusters determined at each time point. Two cells are defined to belong to the same cluster if their distance is smaller than 0.02. The solid line: $b = 0$, dotted line: $b = 5$, dashed line: $b = 15$. Other parameters are the same as in Fig. 3.